A Meticulous Study on the Adsorption of Mercury as Tetrachloromercurate(II) Anion with Trioctylamine Modified Sodium Montmorillonite and Its Application to a Coal Fly Ash Sample

ARTICLE *in* INDUSTRIAL & ENGINEERING CHEMISTRY RESEARCH · AUGUST 2012

Impact Factor: 2.59 · DOI: 10.1021/ie3008693

4 AUTHORS, INCLUDING:

SANTHANA KRISHNA Kumar
National Sun Yat-sen University
28 PUBLICATIONS **268** CITATIONS
SEE PROFILE

Dr. S. Kalidhasan
Weizmann Institute of Science
22 PUBLICATIONS **341** CITATIONS
SEE PROFILE

I&EC research
Industrial & Engineering Chemistry Research

Article

pubs.acs.org/IECR

A Meticulous Study on the Adsorption of Mercury as Tetrachloromercurate(II) Anion with Trioctylamine Modified Sodium Montmorillonite and Its Application to a Coal Fly Ash Sample

A. Santhana Krishna Kumar,[†] S. Kalidhasan,[†] Vidya Rajesh,[‡] and N. Rajesh*,[†]

[†]Department of Chemistry, [‡]Department of Biological Sciences, Birla Institute of Technology and Science, Pilani-Hyderabad Campus, Jawahar Nagar, Shameerpet Mandal, R.R. Dist-500 078(AP), India

ABSTRACT: Clay materials have hogged the limelight for their effectiveness in environmental remediation. In this paper, we report an effective solid phase extraction method for mercury based on the adsorption of tetrachloromercurate(II) anion with trioctylamine intercalated onto sodium montmorillonite. The adsorption is facile in acidic medium, and the adsorbent was well characterized by diverse physicochemical and spectroscopic techniques. Various isotherm models were employed to correlate the experimental adsorption data. The electrostatic interaction between $HgCl_4^{2-}$ and the protonated amine is well supported by a Langmuir isotherm model with a maximum adsorption capacity of 140.84 mg g^{-1}. The ordered transition state that arises due to the proximity of the $HgCl_4^{2-}$ and the positively charged amine is accompanied by a decrease in the translational entropy of the system. The N_2 adsorption−desorption isotherm study revealed the mesoporous nature of the adsorbent, and the thermodynamically favorable adsorption process resonates well with the ensuing negative free energy and enthalpy changes in accordance with the sorption mechanism. Packed bed column study demonstrated the scale up to 800 mL sample volume at 10 mg L^{-1} Hg(II) concentration, and the adsorbent could be regenerated and reused for 10 cycles with thiourea as the eluent. The removal of mercury from a coal fly ash sample validated the method.

1. INTRODUCTION

The indefatigable quest in the journey toward exploring effective adsorbents has witnessed a plethora of methods and materials for the detoxification of heavy metals including mercury.[1] The lacunae with some of the existing adsorbent materials needs to be addressed in terms of the adsorption capacity, regenerability, etc. In this regard, chemically modified clay materials prove to be a viable and attractive alternative as effective adsorbents for toxic heavy metals.[2] Mercury is regarded as one of the most toxic metals in atmospheric and aqueous systems because of its ability to bioaccumulate in the food chain.[3] The pollution of mercury arises from various industrial sources such as coal combustion[4] electronics manufacturing plants, sulfide ore roasting, and chlor-alkali industry.[5] More recently, the concerns due to the pollution of mercury from coal fired utilities has been addressed by USEPA in terms of specifying newer limits with regard to the emission standards.[6] Therefore, effective treatment of the wastewater containing mercury is very important. Many techniques involving liquid−liquid extraction[7] and solid phase extraction[8−10] have been in vogue for the treatment of wastewater containing mercury. Adsorbents such as thiol functionalized clays,[11] silica gel,[12] biomass,[13] thiourea modified chitosan,[14] chitin,[15] barbital immobilized chitosan,[16] silica gel functionalized with amino-terminated dendrimer,[17] rice husk ash,[18] polyaniline/humic acid nanocomposite,[19] thiol-functionalized mesostructured silica,[20] free and monolayer protected silver nanoparticles,[21] and zeolite clusters[22] are known for their efficacy in the removal of mercury. Hollow fiber supported liquid membranes have been studied for the extractive separation of mercury as its tetrachlorocomplex with trioctylamine[23] using sodium hydroxide as the stripping agent. Recently, gold nano particles with citrate as the reducing agent have been reported to adsorb mercury as Au_3Hg on its surface.[24]

The striking properties of clay materials have evoked substantial interest in varied applications. Clays are known for their utility as low cost and well-organized adsorbents in view of their chemical and mechanical stability, high specific surface area, and structural properties. Montmorillonite is a 2:1 clay mineral wherein the layers are held mutually by van der Waals force of attraction.[25] The clays carry a net negative charge, in view of the broken bonds along the edges of Si−Al units which could be offset by the adsorbed cations. The replacement of Al^{3+} and Mg^{2+} for the tetravalent silicon and trivalent aluminum in the tetrahedral and octahedral sheets results in unbalanced charges which makes them serve as fine adsorbents.[26] The montmorillonite clay can be converted quite easily to the sodium form, and, furthermore, the sodium in the interlayer can be exchanged with quaternary ammonium cations thereby imparting organophilicity in the modified form. Intermolecular and surface forces such as van der Waals, hydrogen bonding, ion-dipole, and Coulombic interactions are possible in such organoclays.[27] Organic modifiers are known to have a profound influence on the morphology of clays.[28] In addition to the quaternary ammonium cations such as CTABr,[29] long chain amines such as trioctylamine[30] can also be effectively intercalated in the interlayer of the clays. Thiol ligands loaded onto organophilic sodium montmorillonite have been studied

Received: April 2, 2012
Revised: July 24, 2012
Accepted: August 2, 2012
Published: August 2, 2012

dx.doi.org/10.1021/ie3008693 | *Ind. Eng. Chem. Res.* 2012, 51, 11312−11327

for the voltammetric determination of mercury.[31] The intercalation of protonated pyridinium derivatives in the montmorillonite clay matrix has been utilized in the development of amperometric sensors for mercury.[32] To the best of our literature survey, we have not come across the relevance of trioctylamine modified sodium montmorillonite for the solid phase extraction and detoxification of mercury. In this paper, we report the modification of the sodium form of montmorillonite with trioctylamine and the resulting interaction with mercury followed by its application toward the adsorption and detoxification of mercury from a coal fly ash sample.

2. EXPERIMENTAL SECTION

2.1. Chemicals. Analytical grade reagents were used throughout. The aqueous solutions were prepared in Milli Q water. Montmorillonite was obtained from Fluka. Trioctylamine was procured from Spectrochem, India. Acetone, sulfuric acid, sodium chloride, sodium hydroxide, potassium bromide, potassium iodide, hydrochloric acid, hydrogen bromide, and thiourea were obtained from Merck, India. A 1000 mg L^{-1} stock solution of Hg(II) was prepared from A.R grade mercuric chloride (Merck, India). A working solution of 100 mg L^{-1} Hg(II) as its tetrachloromercurate(II) anion was prepared by appropriate dilution maintaining an overall concentration of 1.0 mol L^{-1} sodium chloride.

2.2. Preparation of Trioctylamine Modified Sodium Montmorillonite. The sodium form of the montmorillonite clay was prepared from montmorillonite as described previously in the literature.[33] An 8.6 mL volume of 0.02 mol of trioctylamine in 3 mol L^{-1} HCl medium was added to 4 g of the sodium montmorillonite suspended in 15 mL of acetone.[34] The acidic medium ensures the protonation of trioctylamine thereby rendering the clay surface organophilic. Further, the contents were stirred magnetically for 10 h. The mixture was centrifuged and washed, and the centrifugate was verified to ascertain the presence of chloride ion by the silver nitrate test. The absence of turbidity in the aqueous phase ensures the complete exclusion of chloride. The amine modified adsorbent material was dried in a hot air oven at 80 °C for 8 h prior to the batch adsorption experiments.

2.3. Batch Adsorption Experiments. The batch experiments were performed by equilibrating 0.2 g of the amine modified clay adsorbent material with a known volume (V) (25 mL of 100 mg L^{-1} Hg(II) solution) at 1.0 mol L^{-1} NaCl concentration adjusted to pH 3.0 in an orbital incubator shaker supplied by Biotechnics, India for varying time intervals, and the concentration of Hg(II) in the solution phase was estimated by the standard Cold Vapor-Atomic Absorption Spectrophotometric (CV-AAS) technique.[35] The amount of mercury adsorbed (q_e) in mg g^{-1} as its tetrachloromercurate(II) anion with the protonated amine was calculated from the difference between the initial concentration of Hg(II), C_o, and the final liquid phase concentration at equilibrium, C_e (both in mg L^{-1}), using the expression

$$q_e = \frac{(C_o - C_e) \times V}{W} \quad (1)$$

where V is the volume of the aqueous solution (L), and W is the weight of the amine modified adsorbent material (g).

2.4. Packed Bed Column Study. For the scale up of the process, a packed bed glass column (3 cm diameter, 30 cm length) was filled with 4.5 g of the amine modified adsorbent. The packing height was fixed at 4 cm. At a flow rate of 8 mL min^{-1} and pH 3.0, a 100 mL volume of 10 mg L^{-1} Hg(II) was transferred to the adsorbent column, and the concentration of mercury in the solution phase was ascertained through CV-AAS technique. The adsorption of mercury as tetrachloromercurate-(II) anion on the packed bed organophilic clay adsorbent column was quantitative (99.4 ± 0.2%), and this was confirmed with three replicate measurements.

2.5. Physico-Chemical Characterization of the Adsorbent Material. The trioctylamine modified onto the montmorillonite clay material in different forms were characterized using various physicochemical characterization techniques. The N_2 adsorption−desorption isotherms were measured at 77 K on a micromeritics porosimeter model ASAP 2020 analyzer. The samples were outgassed at 200 °C for 12 h. The specific surface areas were determined using the Brunauer−Emmett−Teller (BET) method in the relative pressure P/P_o range 0.0−1.0. The pore size distribution curve was obtained using the Barrett-Joyner-Halenda (BJH) model. X-ray diffraction studies were carried out using a Philips PAN alytical X'pert PRO diffractometer with Cu K_α radiation (λ = 0.154 nm) source energized at 40 KV and 30 mA with step size of 0.017°. The samples were scanned at the rate 2.0° min^{-1} in the 2θ range 7° to 60°. The energy dispersive X-ray spectrum was recorded using a Hitachi S-3000H electron microscope. The dry powder samples were coated with a very thin layer of gold prior to recording the spectrum. The FT-IR samples were prepared by mixing 0.01 g of the material with 0.1 g of spectroscopy grade KBr. The FT-IR spectra were recorded in spectral range 400 cm^{-1} to 4000 cm^{-1} using a Jasco-FT-IR-4200 spectrometer. A total of 16 scans were performed (background and sample) at a resolution of 4 cm^{-1}. An Olympus CH20i model optical microscope was used to obtain the images of the adsorbent before and after the adsorption of mercury. The pH adjustments were done using an Elico LI- 127 pH meter (Elico, India). Mercury was analyzed by CV-AAS technique using a mercury analyzer (Model MA 5840, Electronics Corporation of India Ltd. Hyderabad, India).

3. RESULTS AND DISCUSSION

3.1. Characterization of Trioctylamine Modified Sodium Montmorillonite by FT-IR Spectroscopy. In the FT-IR spectrum (Figure 1) characteristic bands corresponding to the various functionalities in the amine modified sodium montmorillonite were observed at 3625 cm^{-1} (ν_{O-H}), 2927 cm^{-1} (ν_{C-H}), 1639 cm^{-1} (δ_{O-H}), 1029 cm^{-1} (ν_{Si-O}), 469 cm^{-1} (ν_{Mg-O}) and 618 cm^{-1} (ν_{Al-O}), respectively.[30,36] The stretching vibrational frequency as a result of the protonation of the tertiary amine (ν_{NH}^{+}) was observed at 2463 cm^{-1}[37] The deformation peak (δ_{N-H}^{+}) in the protonated trioctylamine is obtained at 1377 cm^{-1}.[38,39] After the adsorption of mercury as $HgCl_4^{2-}$, with the positively charged amine, the (ν_{NH}^{+}) shifts to 2484 cm^{-1}. This shift to a higher frequency implies that the tertiary nitrogen in the protonated amine is effective in its interaction with the tetrachloromercurate(II) anion in the clay matrix. The FT-IR study of the adsorbent material indicates that $HgCl_4^{2-}$ (guest) anion is effectively relocated from the aqueous phase to the organophilic clay (host) by means of an interesting host−guest electrostatic interaction with the protonated tertiary amine.

3.2. Surface Morphological Changes and Energy Dispersive X-ray Spectrum of the Adsorbent Material. The surface morphology of the adsorbent material was studied

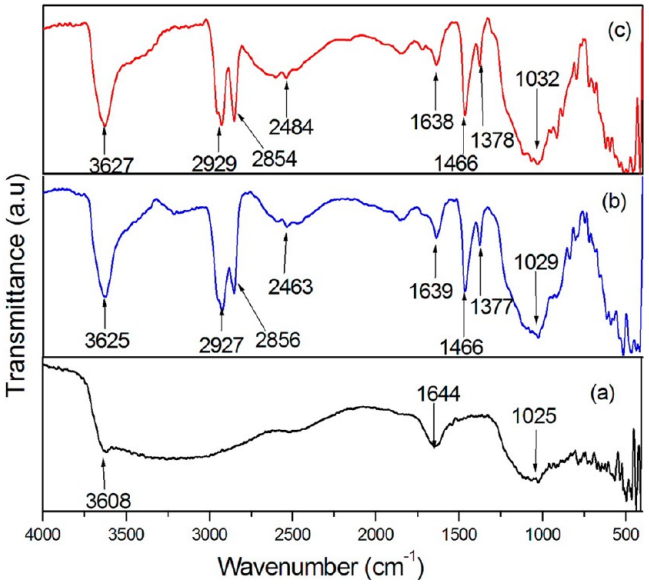

Figure 1. FT-IR spectrum of (a) sodium montmorillonite, (b) trioctylamine intercalated onto the sodium montmorillonite, and (c) adsorbent after the adsorption of mercury.

through the images obtained by optical microscopy. The optical microscopy image for the amine modified adsorbent material (Figure 2a) was obtained by spreading a thin layer of the adsorbent on a glass slide. After the adsorption of Hg(II), a few drops of diphenylthiocarbazone were added as a spot reagent to the adsorbent material, and the image was recorded as mentioned above. Diphenylthiocarbazone is an excellent reagent known to chelate mercury in acidic medium,[40] and the complexation occurs through the sulfur and nitrogen atoms in the ligand. Distinct morphological changes were evident prior and after the adsorption of mercury. The red colored spots (Figure 2b) obtained after adsorption indicates the effective chelation between Hg(II) and diphenylthiocarbazone in acidic medium. The adsorption of mercury on the surface of the trioctylamine intercalated onto the montmorillonite clay was also confirmed through the energy dispersive X-ray (EDX) spectral analysis (Figure 3). The EDX spectrum indicates the presence of adsorbed mercury (in the range 1−2 keV) and other elemental peaks such as C, O, N, Mg, Na, Al, and Si characteristic of the adsorbent at different regions in the spectrum.[41]

3.3. X-ray Diffraction Studies of the Amine Modified Clay Adsorbent. The XRD studies on the adsorbent before and after the adsorption of mercury leads to some interesting observations. Since, an adsorption process might lead to some structural changes in the adsorbent material (in terms of amorphous or crystalline nature), it is vital to assess this phenomenon from the distinct XRD patterns of the adsorbent in various forms. The XRD pattern of sodium montmorillonite prior to the modification with trioctylamine shows sharp and meaningful diffraction peaks at 2θ values (Figure 4a) corresponding to 6.07° (001), 8.99°, 19.81° (100), 25.53°, 26.61°(103), 31.24° and 35.10° (006), respectively.[30,42] After treatment with trioctylamine in acidic medium (Figure 4b), the peaks are shifted to lower 2θ values such as 4.52°, 8.53°, 19.50°, 26.14°, and 34.64°, respectively. This shift could be ascribed to the intercalation the protonated amine in sodium montmorillonite. The XRD pattern of the unmodified clay sample clearly shows reflections corresponding to (001) peak[43,44] at d = 14.92 Å which is characteristic of montmorillonite. After modification with trioctylamine the interlayer spacing increases from 14.92 Å to 20.21 Å. This increase of 5.28 Å is attributed to the effective intercalation of trioctylamine in the clay layer. After the adsorption of mercury as its tetrachloromercurate(II) anion with the protonated amine, the peaks (Figure 4c) sharpen further with a shift in the 2θ values corresponding to 4.8°, 8.87°, and 19.84°, respectively.[45,46] This indicates clearly that there is an effective electrostatic interaction between the protonated amine and the tetrachlorcomplex of mercury in the clay matrix. Furthermore, the sharp peaks also indicate the crystalline nature of the adsorbent material in various forms.

3.4. Surface Area and Barrett-Joyner-Halenda (BJH) Pore Size Distribution. The surface area of the amine modified adsorbent material obtained from N_2 adsorption−desorption study was found to be 20.15 $m^2\ g^{-1}$. This type IV isotherm indicates the mesoporous nature of the adsorbent material (Figure 5a). A pore size of 1.92 nm corresponding to a maximum pore volume of 0.12 $cm^3\ g^{-1}$ was obtained from the Barrett-Joyner-Halenda (BJH) pore size distribution curve (Figure 5b). Literature evidence[47] also points to the fact that

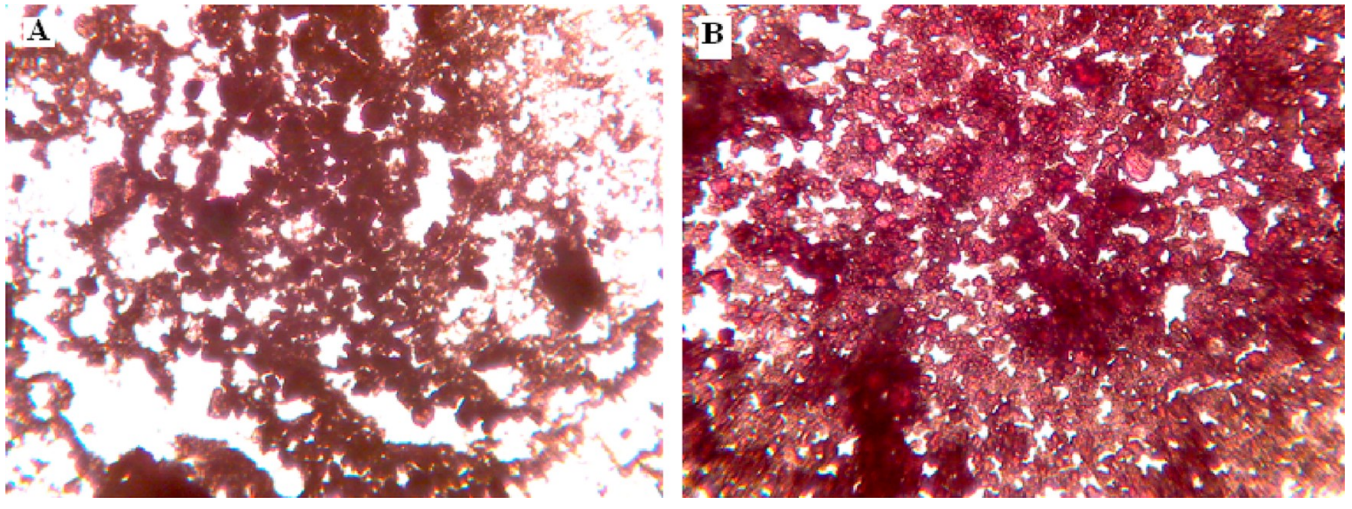

Figure 2. Optical microscopy images: (a) amine modified sodium montmorillonite and (b) after mercury adsorption on the sorbent.

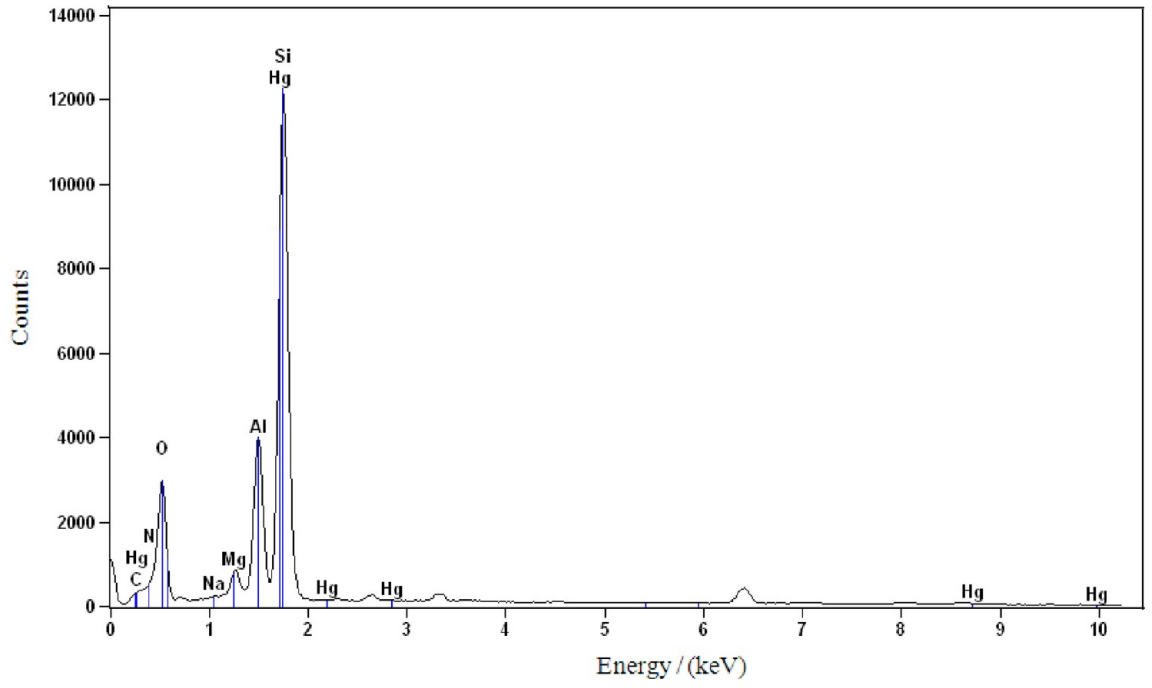

Figure 3. EDX spectrum of the adsorbed mercury on the organophilic clay.

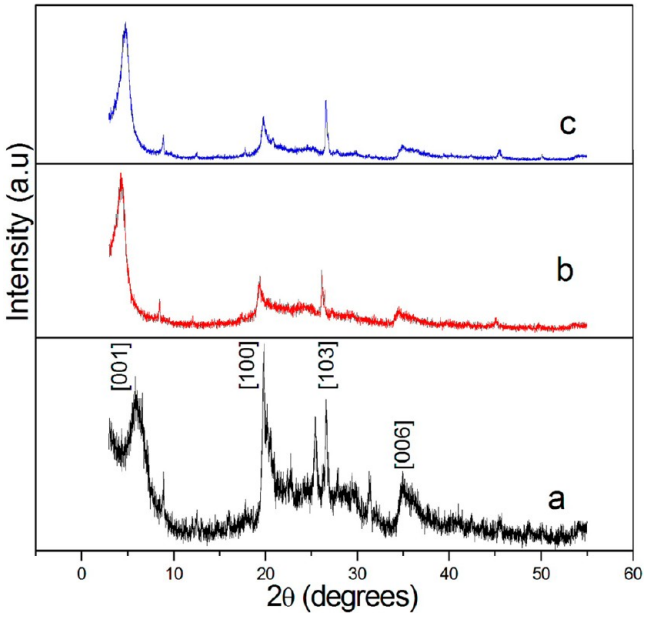

Figure 4. XRD pattern: (a) sodium montmorillonite, (b) amine modified sodium montmorillonite adsorbent, and (c) after mercury adsorption on the sorbent.

ultrastable mesoporous adsorbents as very effective for the removal of mercury ions. This is also corroborated from the supporting evidence such as XRD and EDX spectral analysis which clearly shows the presence of adsorbed mercury on the surface of the adsorbent. Furthermore, the ordered XRD pattern before and after the adsorption of mercury indicates that the mesoporous nature of the adsorbent is retained very well, and hence this could be attributed to the effective interaction of mercury with the adsorbent surface.[47] The mesoporous nature of trioctylamine intercalated onto the montmorillonite clay and the fine surface area indicates the effectiveness in the interaction of tetrachloromercurate(II) anion with the amine modified clay surface.

3.5. pH Dependence and the Mechanism of Adsorption. The optimization of pH is a significant factor in adsorption study. The pH was varied from 2 to 9.5. The favorable pH for the adsorption of Hg(II) was observed in weakly acidic medium (2.5−3.5). Beyond pH 3.5, there is a decrease in the percentage adsorption of mercury. At a concentration greater than 0.5 mol L^{-1} NaCl, the tetrachloromercurate anion is the predominant species.[48] Among the various possible chloro complexes of mercury, the tetrachloro complex has a high stability constant value,[48] and the stepwise formation of the various chloro complexes of mercury with the respective log K (formation constant) values are given below

$$Hg^{2+} + Cl^- \rightleftharpoons HgCl^+ \quad \log K_1 = 6.74 \tag{2}$$

$$Hg^{2+} + 2Cl^- \rightleftharpoons HgCl_2 \quad \log K_2 = 13.22 \tag{3}$$

$$Hg^{2+} + 3Cl^- \rightleftharpoons HgCl_3^- \quad \log K_3 = 14.07 \tag{4}$$

$$Hg^{2+} + 4Cl^- \rightleftharpoons HgCl_4^{2-} \quad \log K_4 = 15.07 \tag{5}$$

It is quite obvious that the fourth step in the above is characterized by a high formation constant value. The selective adsorption of tetrachloromercurate(II) anion in the interlayer of the clay matrix results from an energetically favorable electrostatic interaction between the protonated amine and $HgCl_4^{2-}$ anion.

The silanol groups in the clay surface could be protonated in acidic medium,[49] and this further enhances the electrostatic interaction between tetrachloromercurate(II) anion and the clay surface. In addition, van der Waals interaction could also be possible between the trioctylamine and the clay surface, thereby leading to a good compactness[50] and captivity of $HgCl_4^{2-}$ and the protonated amine in the interlayer. The schematic representation for this interaction is given in Figure 6. Indeed,

dx.doi.org/10.1021/ie3008693 | Ind. Eng. Chem. Res. 2012, 51, 11312−11327

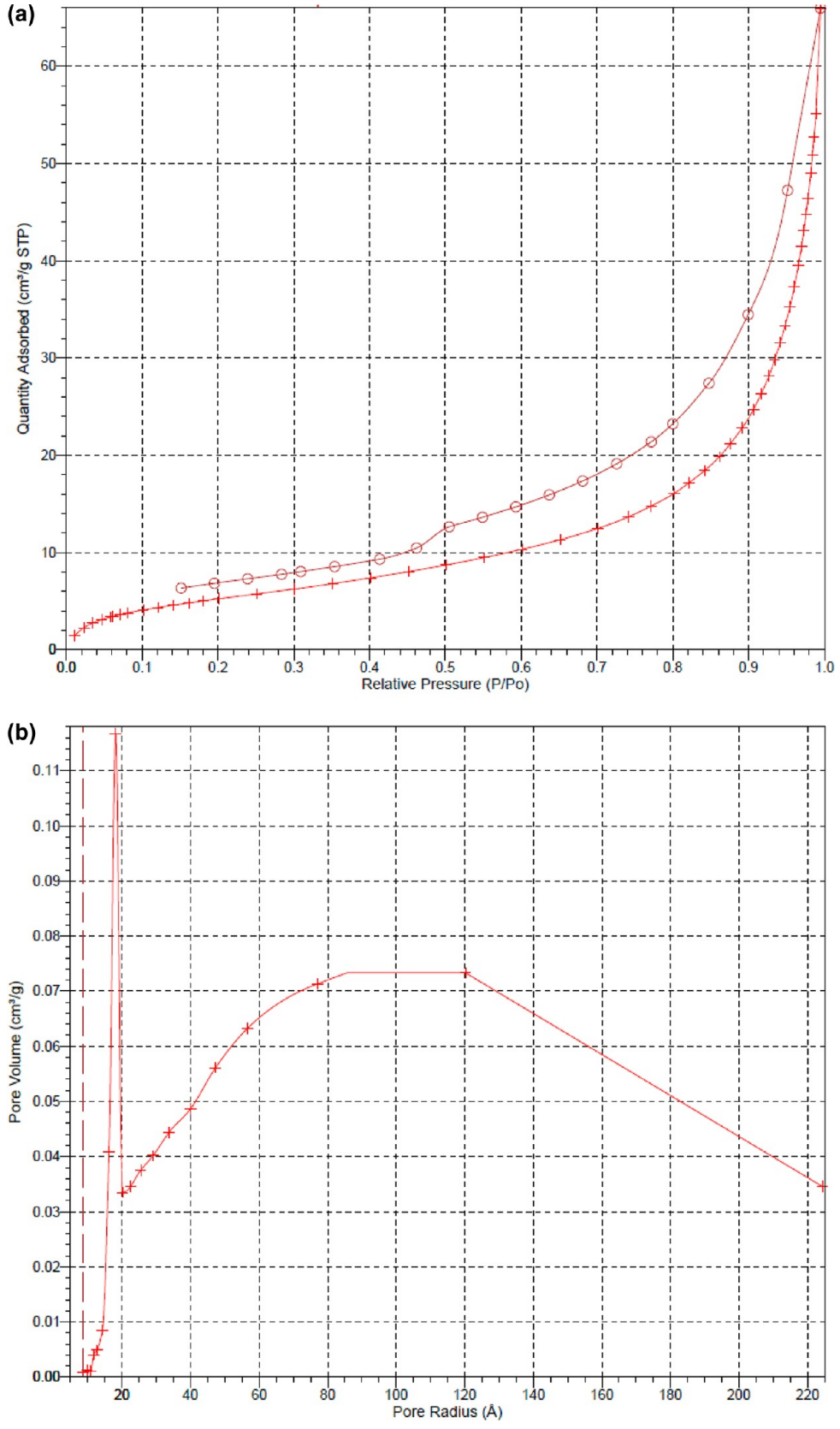

Figure 5. (a) Nitrogen adsorption and desorption isotherm and (b) BJH pore distribution curve.

the organophilic clay matrix acts as an effective host to the guest (i.e., tetrachloromercurate(II) anion) species in the pH range 2.5 to 3.5. At low concentration of chloride (<0.5 mol L^{-1}) and in the pH range 2−5, the predominant mercury species are $HgCl_2$ and $HgCl_3^-$, while the $HgCl_4^{2-}$ anion prevails at chloride concentration (>0.5 mol L^{-1}) in the pH range 2−5. Hg(II) undergoes hydrolysis to HgOHCl and $Hg(OH)_2$ in the pH ranges 6−8 and 9−10, respectively.[51,52] Furthermore, at alkaline

dx.doi.org/10.1021/ie3008693 | *Ind. Eng. Chem. Res.* 2012, 51, 11312−11327

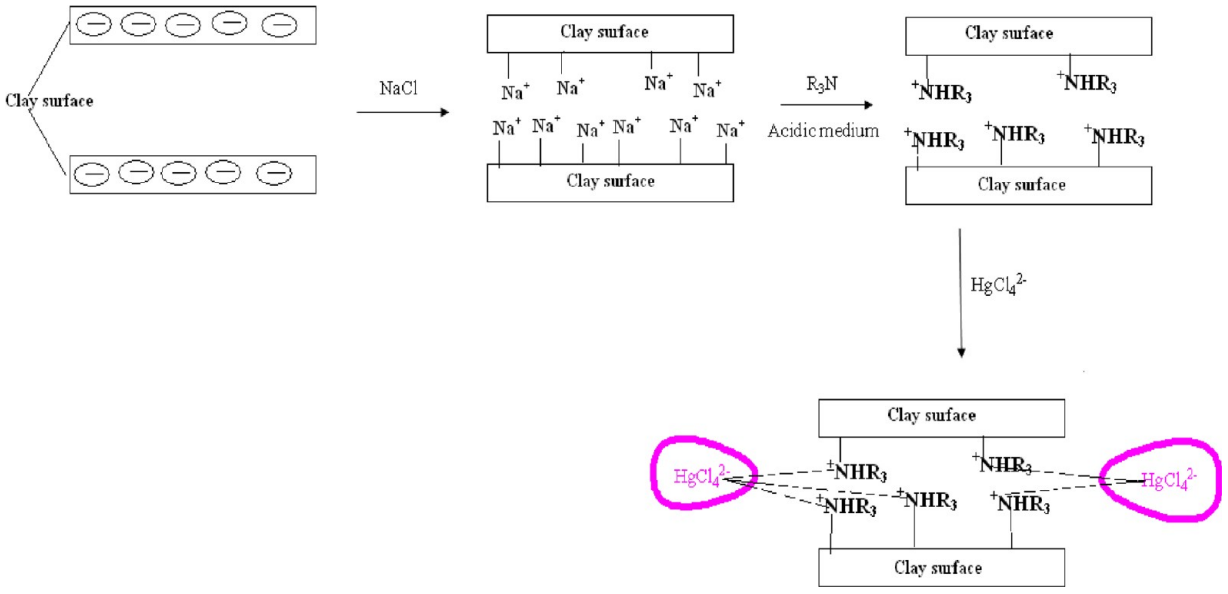

Figure 6. Conceptual illustration showing the interaction of tetrachloromercurate(II) anion with the protonated amine in clay matrix.

pH, formation of $HgOH^+$, $Hg(OH)_2$ species[48] also leads to a reduction in percentage adsorption. The above-mentioned hydroxyl species could compete for the active adsorption species in the clay matrix and hence affect the adsorption of mercury as its anionic tetrachlorocomplex. The pK_a of trioctylamine is 3.5.[53] At pH values< 4, in aqueous acidic medium, the existence of trioctylammonium cation is more favorable. The protonation of amine is facile in the pH range 2−3.5. In basic medium where the pH is greater than pK_a, the amine gets deprotonated, and hence the percentage adsorption of mercury decreases. At pH value greater than 4, the solvation of $HgCl_4^{2-}$ with trioctylamine is more probable and hence the adsorption decreases at higher pH. Tertiary amines are protonated at lower pH values[54] and hence the electrostatic interaction is effective, whereas at higher pH values, the electrostatic repulsion between the anionic chloro complex and the deprotonated amine leads to the decrease in the adsorption of mercury. At higher pH, the deprotonation of the $SiOH^+$ group,[49] in the clay surface as SiO^- might also lead to the decrease in the amount of mercury adsorbed as the tetrachloromercurate(II) anion on the clay surface. The various steps involved in the mechanism could be categorized as a) Protonation of the amine, b) Interaction of the amine with sodium montmorillonite, and c) Adsorption of mercury as its tetrachloromercurate(II) anion. These interactions are illustrated through the following equations:

Step 1: Protonation of trioctylamine

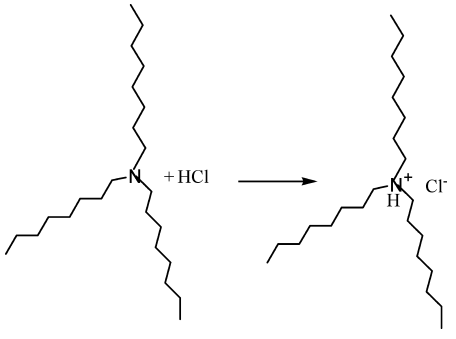

Step 2: Interaction of sodium montomorillonite with protonated trioctylamine

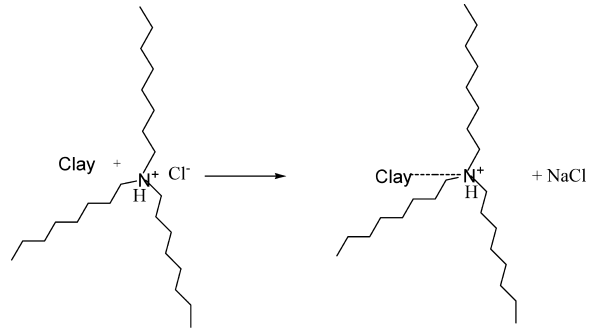

Step 3: Adsorption of mercury in the clay matrix

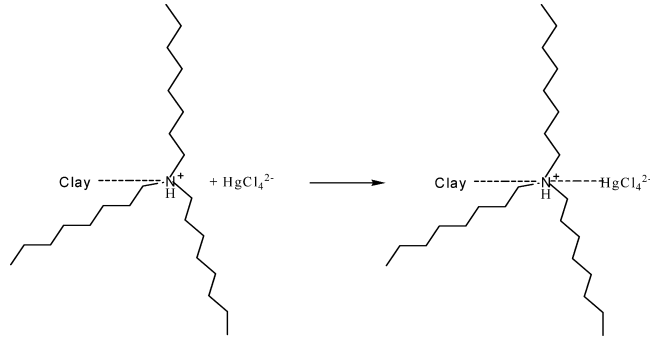

3.6. Effect of the Amount of the Adsorbent Material.

In the batch experiments, the amount of the adsorbent material was varied in the range (0.05 to 0.5) g. The amount of mercury adsorbed as an ion-pair of tetrachloromercurate(II) anion with the protonated amine was found to be maximium (99.2 ± 0.03%) in the range (0.2 to 0.3) g in a 25 mL sample volume. The available adsorption sites and the surface area increases by varying the adsorbent dose and therefore results in the increase in percentage adsorption of mercury. Although, the percentage adsorption increases with an increase in adsorbent dose, the amount of mercury adsorbed per unit mass decreases. This fact is supported from the trend in % adsorption which shows a

dx.doi.org/10.1021/ie3008693 | Ind. Eng. Chem. Res. 2012, 51, 11312−11327

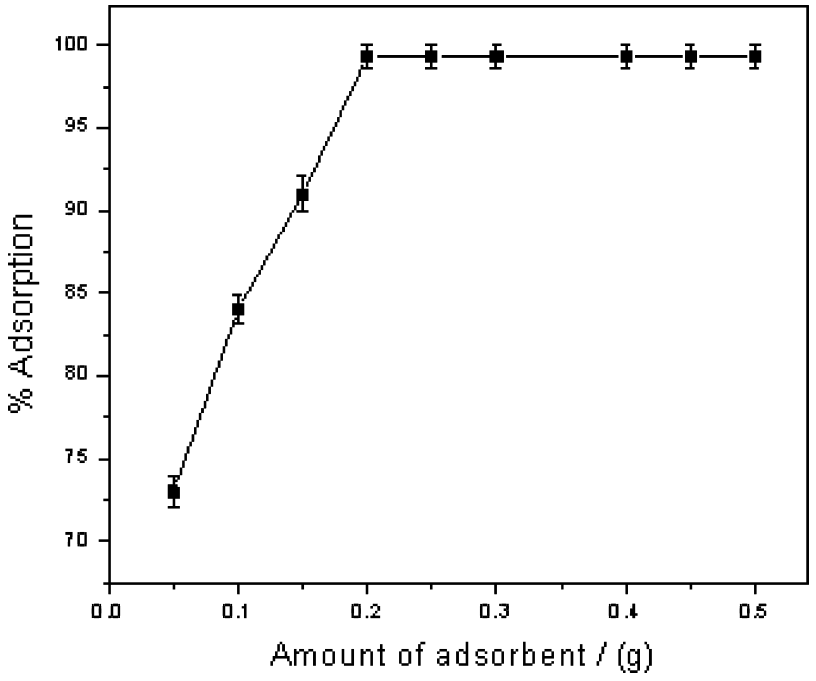

Figure 7. Amount of adsorbent.

sharp increase initially and later attains its maximum at 0.2 g of the adsorbent (Figure 7). The decrease in adsorption capacity with an increase in adsorbent dose is attributed to unsaturation of adsorption sites in the process of adsorption.[55]

3.7. Study of Various Isotherm Models. The adsorption process is best described through various isotherms which relate the amount of the adsorbate to the concentration. A variety of isotherm models was employed to study the effectiveness of the adsorbent−adsorbate interaction. Langmuir isotherm[56] is one of the commonly used empirical isotherm models which take into account the uniformity in the adsorbent surface with a monolayer. The adsorption of $HgCl_4^{2-}$ from the bulk onto the surface of the organophilic clay matrix can be expressed by the linearized Langmuir isotherm expression as

$$\frac{C_e}{q_e} = \frac{1}{q_o b} + \frac{C_e}{q_o} \tag{6}$$

From the plot of C_e/q_e against C_e, the maximum adsorption capacity, q_o (mg g^{-1}), of Hg(II) and the constant b are obtained from the slope and intercept, respectively. The constant b is attributed to the affinity between the amine modified adsorbent and mercury(II). These isotherm parameters are given in Table 1. Furthermore, the Langmuir isotherm model also relates a dimensionless parameter R_L to the concentration of mercury C_o and b as

$$R_L = \frac{1}{1 + bC_o} \tag{7}$$

The R_L value has considerable importance when it lies between 0 and 1, where it implies an effective interaction between the adsorbent and the adsorbate. The values greater than 1 are an indication of an unfavorable isotherm, and R_L equal to zero is accounted for a totally irreversible isotherm.[57] In the present system, the R_L value is obtained in the range 0−1 (0.0848, C_o = 100 mg L^{-1}), and this implies that there is a strong interaction between the tetrachloromercurate(II) anion and the protonated amine in the clay matrix. This favors an enhanced adsorption by way of effective adsorbent−adsorbate (host−guest) interaction. The obtained b value reiterates the above as regards the effectiveness of the adsorbent−adsorbate interaction.

Another extensively employed empirical isotherm model to study the adsorption process from aqueous solution is the Freundlich model which relates q_e and C_e given by the linearized expression as[58]

$$\log q_e = \log K_F + \frac{1}{n}\log C_e \tag{8}$$

In this expression, the constants K_F and n indicate the adsorption capacity and adsorption intensity, respectively. This model is based on multilayer adsorption. At low concentration of the adsorbate, the extent of adsorption varies linearly with concentration, whereas at higher levels it becomes independent of the concentration. A good adsorbent material is characterized by n value in the range 1−10. A higher value of n indicates better adsorption and formation of relatively strong adsorbent−adsorbate interaction. From the slope and intercept obtained through the logarithmic plot of q_e against C_e, the constants K_F and n were found to be 16.95 $mg^{1-1/n}$ g^{-1} $L^{1/n}$ and 1.806, respectively (Table 1).

3.7.1. Dubinin−Radushkevich (D-R) Isotherm. The adsorption mechanism and the interaction between mercury and the amine modified adsorbent surface can be understood through yet another isotherm model known as the Dubinin−Radushkevich isotherm.[59] Although, this model is somewhat comparable to the Langmuir isotherm, the D-R model does not take into account a steady adsorption potential. The D-R isotherm is best expressed in the linearized form as

$$\ln q_e = \ln q_m - \beta\varepsilon^2 \tag{9}$$

where q_e is the amount of mercury(II) adsorbed at equilibrium (mg g^{-1}), q_m is the maximum adsorption capacity, and the constant β relates to the adsorption energy; ε is another important parameter better known as the Polanyi potential, and

dx.doi.org/10.1021/ie3008693 | Ind. Eng. Chem. Res. 2012, 51, 11312−11327

Table 1. Adsorption Isotherm Parameters

Sl. no.	isotherm model	parameters	values
1	Langmuir	q_o (mg g^{-1})	140.84
		b (L mg^{-1})	0.1079
		R_L	0.0848
		r^2	0.98
		p	0.0001
		SD	0.0122
		APE (%)	7.2
2	Freundlich	K_F (mg $^{1-1/n}$ g^{-1} $L^{1/n}$)	16.95
		n	1.806
		r^2	0.98
		p	0.0001
		SD	0.0475
		APE (%)	8.4
3	Dubinin−Radushkevich	q_m (mg g^{-1})	63.41
		β (mol^2 kJ^{-2})	0.3299
		E (kJ mol^{-1})	1.23
		r^2	0.63
		p	0.0172
		SD	0.5417
		APE (%)	45.2
4	Redlich Peterson	g	0.845
		B (L mg^{-1})	0.2025
		A (L g^{-1})	15.196
		r^2	0.74
		p	0.0118
		SD	0.6944
		APE (%)	18.69
5	Temkin	B	26.280
		A (L mg^{-1})	1.595
		b (J $mole^{-1}$)	94.27
		r^2	0.96
		p	0.0001
		SD	8.2148
		APE (%)	23.9
6	Elovich	q_m (mg g^{-1})	60.35
		K_E (L mg^{-1})	0.337
		r^2	0.96
		p	0.0001
		SD	0.5417
		APE (%)	25.74

this factor relates the equilibrium concentration of mercury(II) to the gas constant R and temperature T as

$$\varepsilon = RT \ln\left(1 + \frac{1}{C_e}\right) \tag{10}$$

The slope and intercept of the plot of ln q_e versus ε^2 gives the parameters β and q_m (Table 1). Further, the mean free energy E_{DR} (kJ mol^{-1}) of adsorption and the constant β can be related through the expression

$$E_{DR} = 1/(2\beta)^{-0.5} \tag{11}$$

The nature of the adsorption mechanism is ascertained from the E_{DR} values. The mean free energy value lower than 8 kJ mol^{-1} is indicative of physical adsorption. In the present system, involving the electrostatic interaction between tetrachloromercurate(II) anion and the organophilic clay surface, a value of 1.23 kJ mol^{-1} was obtained, and this is attributed to the physical adsorption.

3.7.2. Redlich−Peterson (R-P) Isotherm. A three parameter isotherm known as the R-P model includes the attributes of Langmuir and Freundlich isotherms. The Redlich−Peterson model relates the constants A and B and an exponent g to the amount of mercury adsorbed at equilibrium q_e by the equation[60]

$$q_e = AC_e/1 + BC_e^g \tag{12}$$

It has been observed in many adsorption systems that the value of g lies between 0 and 1. Indeed, when g = 1, the above expression simplifies to the simple Langmuir equation.[61] The characteristic isotherm parameters were obtained from the linearized form the above equation expressed as

$$\ln(AC_e/q_e - 1) = g \ln(C_e) + \ln(B) \tag{13}$$

The slope and intercept of the plot gives the parameters g and B, respectively (Table 1). The value of g was found to be 0.845 (near to 1), and this shows that the system could adhere to the Langmuir isotherm model.

3.7.3. Temkin Isotherm. The Temkin isotherm model is based on the assumption that the adsorption energy decreases linearly with the surface coverage. The Temkin isotherm is best expressed as[62,63]

$$q_e = \frac{RT}{b}\ln A + \frac{RT}{b}\ln C_e \tag{14}$$

where RT/b = B. The linear plot of q_e versus ln C_e gives the constants A and B. The variation of adsorption energy and the Temkin equilibrium constant can be calculated from the slope and the intercept of the plot q_e versus ln C_e, and the respective isotherm parameters are given in Table 1.

3.7.4. Elovich Isotherm. The Elovich model[64,65] is based on the fact that the adsorption sites increase exponentially with adsorption, thereby leading to a multilayer adsorption. The Elovich equation is expressed in linearized form as

$$\ln\left(\frac{q_e}{C_e}\right) = \ln(K_E q_m) - \frac{q_e}{q_m} \tag{15}$$

where K_E is the Elovich equilibrium constant (L mg^{-1}), and q_m is the Elovich maximum adsorption capacity (mg g^{-1}). The respective isotherm parameters can be obtained from the slope and the intercept of the plot ln (q_e/C_e) against q_e, and these are given in Table 1.

3.7.5. Statistical Treatment of the Individual Isotherm Models. The suitability of an isotherm model to understand the present adsorption system is best assessed through the statistical analysis of the experimental and calculated data obtained through the various isotherm models. Regression coefficient (r^2) is one parameter which helps us to find out the fit to the best possible model. However, this needs to be substantiated by calculating the average percentage error (APE) in each of these isotherm models. The APE is essentially the standard deviation which takes into account the difference in the summation of the experimental and calculated q_e values and the number of experimental data points, N. The APE can be expressed mathematically[66] as

$$\mathrm{APE}(\%) = \frac{\sum_{i=1}^{N} |((q_e)_{exptl} - (q_e)_{calcd})/(q_e)_{exp\ tl}|}{N} \times 100 \tag{16}$$

dx.doi.org/10.1021/ie3008693 | Ind. Eng. Chem. Res. 2012, 51, 11312−11327

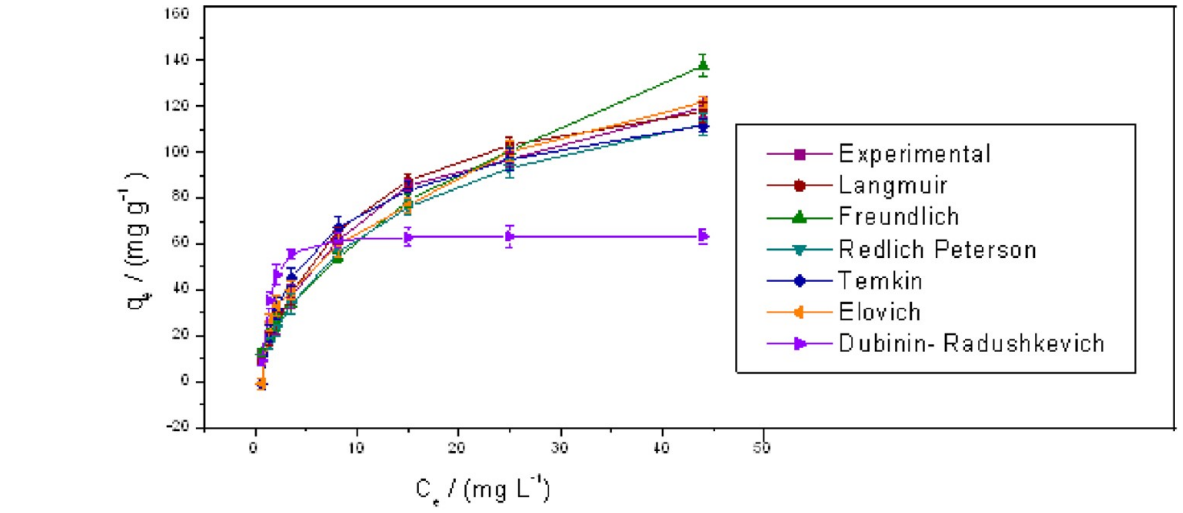

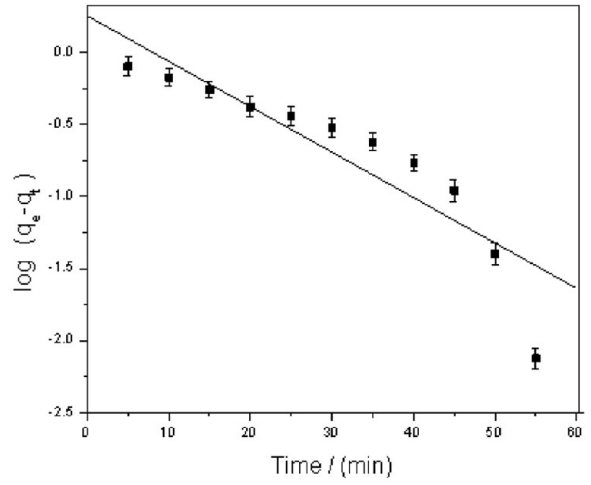

(b) Pseudo first order kinetic plot

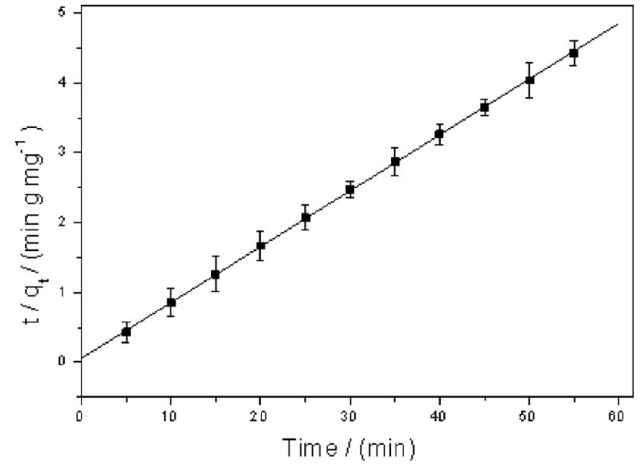

(c) Pseudo second order kinetic plot

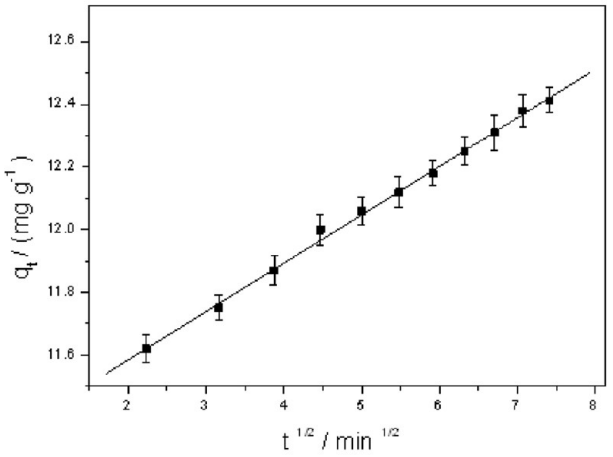

(d) Plot of q_t against square root of time

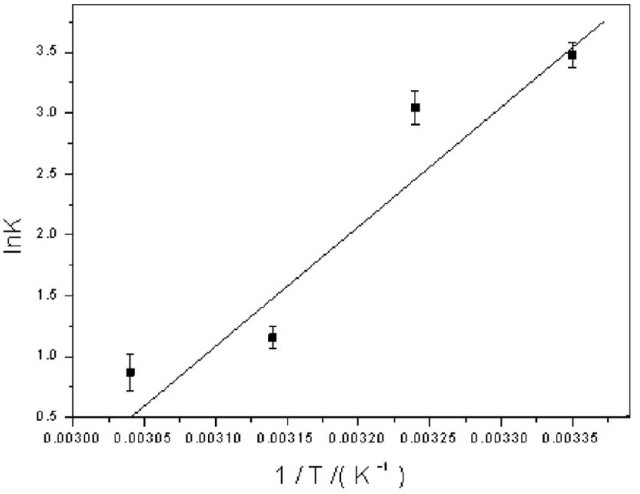

(e) Van't Hoff plot showing the variation of lnK against reciprocal of temperature.

Figure 8. (a) Plot of q_e against C_e, (b) pseudo first order kinetic plot, (c) pseudo second order kinetic plot, (d) plot of q_t against square root of time, and (e) Van't Hoff plot showing the variation of ln K against reciprocal of temperature.

The regression coefficient in the case of Langmuir and Freundlich models was close to 1 (0.98), and the APE in the case of the above isotherm models were found to be 7.2 and 8.4%, respectively. The lower APE indicates good adherence to the Langmuir model, and, furthermore, the respective isotherm data plots of q_e against C_e which is L shaped in accordance with

dx.doi.org/10.1021/ie3008693 | *Ind. Eng. Chem. Res.* 2012, 51, 11312−11327

Table 2. Kinetic Parameters for the Adsorption of Mercury(II)

C_o (mg·L^{-1})	q_e (mg g^{-1})	second order rate constant (k_2/(g mg^{-1} min^{-1}))	regression coefficient (R_1^2)	p	standard deviation	first order rate constant (k_1/(min^{-1}))	regression coefficient (R_2^2)	p	standard deviation
100	12.48	0.1175	0.99	0.0001	0.0175	0.0108	0.90	0.0001	0.2697

Giles classification[67] also shows a better fit to the Langmuir isotherm in terms of the good proximity to the experimental and calculated data points (Figure 8a). Moreover, the maximum adsorption capacity for mercury (140.84 mg g^{-1}) was obtained in the case of the Langmuir isotherm model. The APE in the other isotherm models was quite large and with lower correlation coefficient values. The level of significance of regression coefficient is also given by the p value and the standard deviation. The p value gives a clue as to how likely it is for the coefficient of an independent variable to emerge by chance. In general as an accepted practice, a p value of less than 0.1 is considered as significant. The significance of the adsorption data is very well illustrated from the p values and the standard deviation given in Table 1. Taking into cognizance all these observations, the Langmuir isotherm model seems to be superlative for the data obtained in the study of the interaction between the tetrachlorocomplex of mercury and the protonated amine in the clay matrix.

3.8. Adsorption Kinetics. The adsorption data were fitted to the first order and pseudo second order kinetic equations. These equations relate the amount of mercury adsorbed q_t at time t and at equilibrium q_e as given by the following expressions[68,69]

$$\log (q_e - q_t) = \log q_e - \frac{k_1 t}{2.303} \tag{17}$$

$$\frac{t}{q_t} = \frac{1}{k_2 q_e^{\,2}} + \frac{t}{q_e} \tag{18}$$

The plot of log (q_e−q_t) against t (Figure 8b) and t/q_t against t (Figure 8c) gives the kinetic parameters. The experimental data show a good fit to the pseudo second order model owing to the higher regression coefficient value. In addition, the chi square value obtained from the second order model was found to be lower as compared to the first order kinetic data. Furthermore, the $q_{e\ calcd}$ and $q_{e\ exptl}$ values were found to be 12.48 mg g^{-1} and 12.40 mg g^{-1} in agreement with the second order model. This proximity in the values (Table 2) further confirms the suitability of the second order kinetics to the adsorption data. The p value and the standard deviation also support the significance of the second order model.

3.8.1. Intraparticle Diffusion. The transport of the tetrachloromercurate(II) anion from the solution phase to the surface of the adsorbent could be controlled by film or external diffusion, pore and surface diffusion.[70] In addition, there is also a likelihood of intraparticle diffusion of the metal ion from the bulk into the pores of the adsorbent material, which is generally a slow process. The intraparticle diffusion is studied using the well-known Weber Morris[71] intraparticle diffusion model, which relates the amount of Hg(II) adsorbed at time t to the intraparticle diffusion rate constant k_{int}

$$q_t = k_{int}\sqrt{t} + C \tag{19}$$

The constant C is indicative of the thickness of the boundary layer. A plot of q_t vs $\sqrt{t}$ gives a straight line (Figure 8d), and the intraparticle rate constant as obtained from the slope was found to be 0.155 mg g^{-1} min$^{-1/2}$. Since, q_t increases with the time of adsorption t, initially the external surface diffusion could influence the kinetics followed by intraparticle diffusion as the rate-determining step.[72] The Weber-Morris plot does not pass through the origin, and hence we can conclude that in addition to intraparticle diffusion, the boundary layer effect[39] also could influence the kinetics in the adsorption of the tetrachloromercurate(II) anion in the interlayer of the organophilic clay matrix.

3.9. Thermodynamics of Adsorption. The thermodynamics of adsorption were studied at 298, 308, 318, and 328 K, respectively, in order to obtain the Gibb's free energy (ΔG^0), enthalpy (ΔH^0), and entropy (ΔS^0) changes in the overall process. These parameters are obtained through the classical Van't Hoff equations[73]

$$\Delta G^0 = -RT \ln K \tag{20}$$

$$\ln K = \frac{-\Delta H^0}{RT} + \frac{\Delta S^0}{R} \tag{21}$$

The equilibrium constant K is obtained from the ratio of concentration of Hg(II) adsorbed on the amine modified adsorbent to that in the solution. The endothermic or exothermic nature of the adsorption process is reflected through the positive and negative values of ΔH^0. The thermodynamic parameters, ΔH^0 and ΔS^0, were obtained from the slope and intercept of the plot of ln K against 1/T (Figure 8e). The negative values of ΔG^0 imply a spontaneous physical adsorption process, and the respective thermodynamic parameters are given in Table 3. The negative free energy

Table 3. Thermodynamic Parameters for the Adsorption of Mercury

temperature (Kelvin)	concentration (mg L^{-1})	ΔG^0 (kJ mol^{-1})	ΔS^0 (J mol^{-1} K^{-1})	ΔH^0 (kJ mol^{-1})
298	100	−8.612	−233.15	−78.09
308	100	−5.225		
318	100	−3.04		
328	100	−2.37		

(ΔG^0) values confirm the effectiveness of the electrostatic interaction between $HgCl_4^{2-}$ and the protonated amine. The overall free energy of adsorption (ΔG_{ads}) could arise from a combination of this electrostatic force of attraction as well as possible interaction between the positively charged amine and the oxygen framework in the clay surface

$$\Delta G_{adsorption} = \Delta G_{electrostatic} + \Delta G_{van\ der\ Waals} \tag{22}$$

The fact that ΔH is negative is an interaction of the exothermic nature of adsorption and enthalpy factor is predominant at lower temperature than the entropy. The adsorption is enthalpically more favorable at lower temperature, and this is also obvious from the free energy values obtained at these temperatures. The ΔG^0 values decrease with an increase in temperature (298−328 K) with negative entropy and enthalpy changes during the adsorption process. The overall

dx.doi.org/10.1021/ie3008693 | Ind. Eng. Chem. Res. 2012, 51, 11312−11327

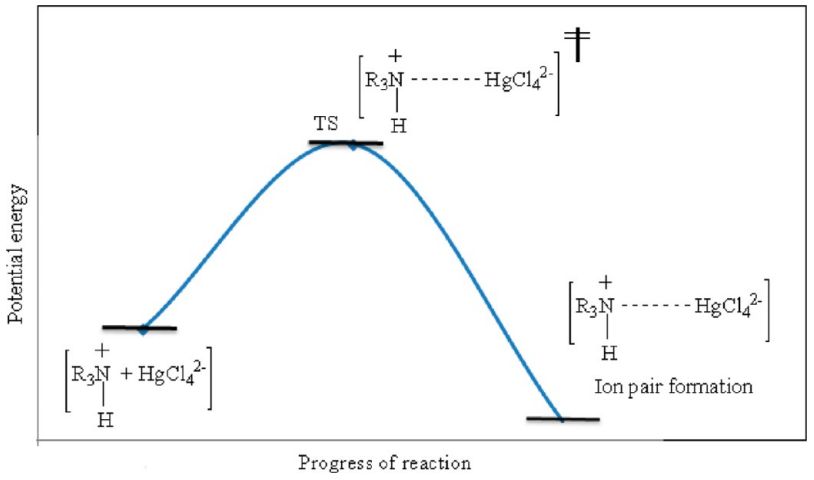

Figure 9. Energy profile of the ion-pair formation.

enthalpy and entropy of adsorption could be visualized as a summation of the enthalpy and entropy due to the amine modified clay and the tetrachloromercurate(II) anion.[74]

$$\Delta H_{adsorption} = \Delta H_{(amine\ modified\ clay)} + \Delta H_{HgCl4}{}^{2-} \quad (23)$$

$$\Delta S_{adsorption} = \Delta S_{(amine\ modified\ clay)} + \Delta S_{HgCl4}{}^{2-} \quad (24)$$

$$\Delta G_{adsorption} = \Delta H_{adsorption} - T(\Delta S_{amine\ modified\ clay} + \Delta H_{HgCl4}{}^{2-}) \quad (25)$$

As a matter of fact, these enthalpy and entropy factors play an interesting role in ion-pair interactions.[50] Since $\Delta G < 0$, $\Delta S < 0$, and $\Delta H < 0$, with $K > 1$, $T < \Delta H_{ads}/\Delta S_{ads}$ and hence in accordance with the Le-Chatlier principle, an increase in temperature would not favor the adsorption process (as the process is exothermic). When $HgCl_4^{2-}$ and the positively charged amine come in proximity to form an ordered transition state, there is a decrease in the translational entropy of the system

$$HgCl_4{}^{2-} + R_3\overset{+}{N}H \rightarrow [HgCl_4{}^{2-}\text{----------}R_3\overset{+}{N}\text{-}H]^{\ddagger} \rightarrow HgCl_4{}^{2-}\text{--------}R_3\overset{+}{N}\text{-}H \quad (26)$$

This could also be schematically illustrated by plotting the potential energy against the progress of the reaction (Figure 9). This leads to the decrease in randomness at the solid solution interface, with decrease in the activation energy barrier and the interionic distance.[50] It is this sort of compactness that eventually results in negative entropy change during the adsorption process. The permeation of the tetrachloromercurate(II) anion from the bulk to the interlayer of the clay matrix results in strong electrostatic interaction with the positively charged amine.

The ability of the tetrachloromercurate(II) anion to permeate the headgroup ($-N^+H$) of trioctylamine is also in accordance with the Hofmeister series[75] for simple anions ($Cl^- > NO_3^- > Br^- > I^-$). The Hofmeister series for anions play an important role in understanding the effective interaction with the surrounding water molecules. Multiple charged ions with high charge density such as $HgCl_4^{2-}$ are classified as kosmotropic[76] and are well hydrated, whereas singly charged large size ions are chaotropic and are poorly solvated. In this regard, even though the long chain protonated trioctylamine is singly charged (R_3N^+H), and bulky, it is not really chaotropic in view of its hydrophobic hydration.[76] As a result, we can visualize the amine species to exhibit certain degree of kosmotropicity as well. Kosmotropes, being structure makers,[76] have good interaction with water molecules, resulting in negative $\Delta S_{hyd.}$ Furthermore, the entropy of hydration also includes the contribution from electrostatic and van der Waals interaction

$$\Delta S_{hyd} = \Delta S_{electrostatic} + \Delta S_{van\ der\ Waals} \quad (27)$$

$$\Delta S_{ads} = \Delta S_{electrostatic} + \Delta S_{hyd} + \Delta S_{van\ der\ Waals} \quad (28)$$

Hence, in addition to the strong electrostatic interaction between $HgCl_4^{2-}$ and the protonated amine, the tetrachloromercurate(II) anion and the kosmotropic amine are also solvated or hydrated which leads to a considerable order thereby resulting in a negative entropy change. The van der Waals interaction of the ions with the solvent also affect the entropy change in the adsorption process. At low temperatures, the tetrachloromercurate(II) anion could be solvated effectively. Nevertheless, as a trade of between solvation and electrostatic interaction, effectiveness of ion-association between the $HgCl_4^{2-}$ and the protonated amine is of considerable importance in the adsorption mechanism. The chain length of alkylamine is also an important factor[50] that causes this entropy change arising as a result of the protonation of the amine. Hence, the interplay of solvation effect and electrostatic interaction fosters good interaction for the effective adsorption of Hg^{2+} as its tetrachloromercurate(II) anion in the clay matrix.

This leads to a negative entropy change during the adsorption process. The fact can be further substantiated by considering the free energy changes associated with sodium montmorillonite, trioctylamine (TOA), and tetrachloromercurate(II) anion, respectively. The change in the free energy can be expressed as the difference in the enthalpy and the entropy changes of the respective components as follows

$$\Delta G_{(sodium\ form\ clay)} = \Delta H_{(sodium\ form\ clay)} - T\Delta S_{(sodium\ form\ clay)} \quad (29)$$

$$\Delta G_{TOA} = \Delta H_{TOA} - T\Delta S_{TOA} \quad (30)$$

$$\Delta G_{HgCl4}{}^{2-} = \Delta H_{HgCl4}{}^{2-} - T\Delta S_{HgCl4}{}^{2-} \quad (31)$$

dx.doi.org/10.1021/ie3008693 | Ind. Eng. Chem. Res. 2012, 51, 11312−11327

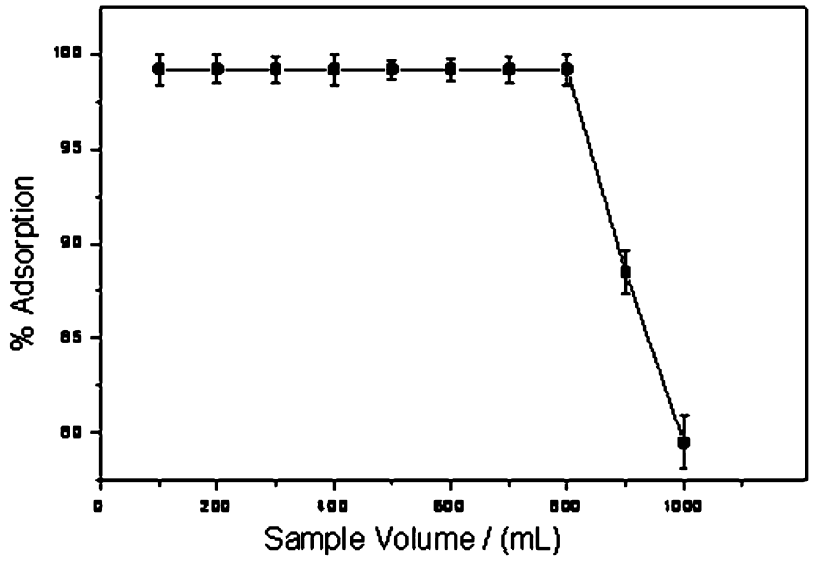

Figure 10. Sample breakthrough volume study.

$$\Delta G_{adsorption} = \Delta H_{adsorption} - T(\Delta S_{(sodium\ form\ clay)} + \Delta S_{TOA} + \Delta S_{HgCl4}{}^{2-}) \quad (32)$$

The interaction of the protonated amine (NH^+) with the negatively charged tetrachloromercurate ion is characterized by a negative value of enthalpy and entropy. The overall entropy contribution arises from the individual entropy changes disassociated with the clay and amine. Hence, the summation, $\sum(\Delta S_{(sodium\ form\ of\ clay)} + \Delta S_{TOA} + \Delta S_{HgCl\ 4}{}^{2-})$ becomes largely negative reflecting the decreased randomness at the adsorbent-solution interface. Overall, the physicochemical adsorption process is enthalpy driven rather than the entropy effect. The average energy of activation, obtained from the expression[74] $E_a = \Delta H_{ads} + RT$, was found to be −75.48 kJ mol^{-1}; this indicates the exothermic nature of adsorption.

3.10. Effect of Sample Breakthrough Volume in Column Study. Clays are known to swell or expand when they are in contact with aqueous solution, and the extent of swelling is dependent on the sample volume. The adsorption of Hg(II) is quantitative up to a 800 mL sample volume (Figure 10) at 10 mg L^{-1}concentration of Hg(II). Above 800 mL, there is a decrease in the percentage adsorption of mercury. This could be attributed to a considerable expansion in the packed bed column,[39,74] and, as a consequence, the close packing of the adsorbent is disturbed in the column. Hence, the retention of mercury as its tetrachloromercurate(II) anion with the protonated amine in the column is not quantitative beyond the 800 mL sample volume. As low as 10 ppb of mercury could be adsorbed effectively in the column. Furthermore, the adsorption is also quantitative at an optimized flow rate of 8 mL min^{-1} which ensures effective contact between the mercury(II) and the adsorbent. The performance of an adsorbent is also expressed in terms of the rate at which the adsorbent bed gets exhausted. The rate of exhaustion of the adsorbent bed is given by the ratio of the mass of the adsorbent to the maximum sample volume.[77] On a laboratory scale, with 4.5 g of the adsorbent, at 10 mg L^{-1} concentration of Hg(II), the exhaustion rate of the adsorbent is 5.6 g L^{-1}. A lower value of the exhaustion rate signifies the effectiveness of the adsorbent column. Hence, it is possible that on an industrial scale, with an increase in the amount of the adsorbent in the column, the upper limit for the sample volume would also enhance correspondingly.

3.11. Desorption Studies. The regeneration of adsorbent is an important aspect to be examined in an adsorption process. A 100 mL volume of 10 mg L^{-1} Hg(II) was loaded on the adsorbent column at a flow rate of 5 mL min^{-1}. The desorption of mercury was studied individually using 15 mL of 1.0 mol L^{-1} of potassium iodide, potassium bromide, and hydrogen bromide, respectively. Bromide and iodide are known to form stable tetraiodo and tetrabromo complexes[78] and hence compete with tetrachloromercurate(II) anion for the effective sites in the adsorbent matrix as well as the protonated amine. In view of the competing ability of these two halides with chloride for the protonated amine the adsorption of mercury in the column is affected, and hence it is probable that some amount of mercury could be released in the aqueous phase. Furthermore, in aqueous solution the E^o (standard reduction potential) of I_2/I^-, Br_2/Br^-, and Cl_2/Cl^- are +0.54 V, +1.09 V, and +1.36 V, respectively.[79] Hence, in aqueous acidic medium it is also highly probable that bromide and iodide can be oxidized easily and hence elute the mercury also as covalent HgI_2 and $HgBr_2$ in the aqueous phase. As a result, the interaction of tetraiodo and tetrabromo complexes with the protonated amine is not quantitative as compared to the tetrachloromercurate(II) anion. This leads to the partial elution of mercury with bromide and iodide into the aqueous phase. Since, bromide and iodide were not effective in quantitative elution, thiourea was tried as an alternative organic complexing agent for mercury(II). In the proposed methodology, we found that 10 mL of 2.0 mol L^{-1} thiourea was effective in quantitative desorption (99 ± 0.3%) of mercury in the eluate. Although, the tetrachloromercurate(II) anion has a high stability constant (log K = 15.07), the addition of thiourea leads to a weakening of interaction between $HgCl_4^{2-}$ and the adsorbent. Since Hg^{2+} is a typical soft acid, it has very good affinity toward sulfur containing ligands like thiourea.[80−82] Thiourea forms a 1:2 complex with Hg(II), thereby bringing down the mercury to the aqueous phase and regenerating the adsorbent (Figure 11). The order of elution with the above tested reagents were found to be thiourea (99.3%) > potassium iodide (79%) > potassium

dx.doi.org/10.1021/ie3008693 | Ind. Eng. Chem. Res. 2012, 51, 11312−11327

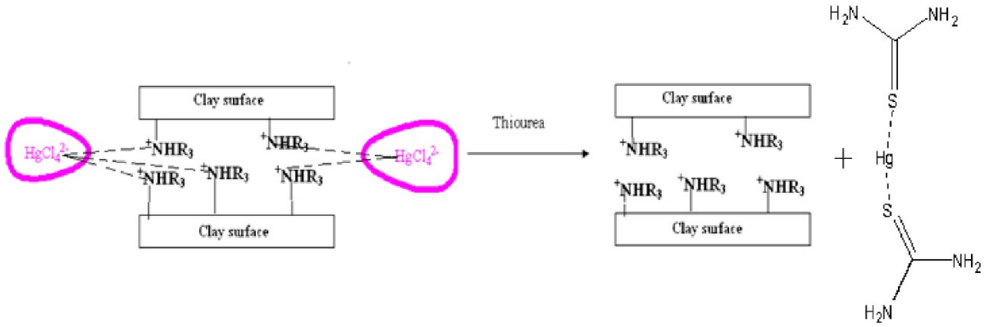

Figure 11. Regeneration of adsorbent.

bromide (62%) > hydrogen bromide (49%). The adsorbent could be reused for 10 adsorption−desorption cycles without any noticeable decrease in the performance efficiency of the column.

3.12. Impact of Coexisting Ions. The effect of diverse ionic constituents (Figure 12) was investigated in order to

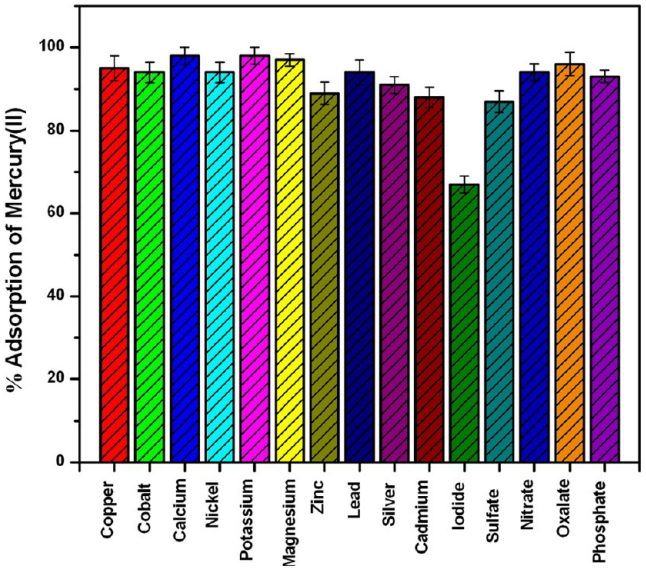

Figure 12. Effect of diverse ionic constituents.

study their impact on the adsorption efficiency of mercury. A 100 mL volume of 10 mg L^{-1} Hg(II) was mixed individually with varying concentrations of these ions and loaded on the column. The amount of mercury adsorbed was ascertained to study the extent of interference of these species. At lower concentration (150 mg L^{-1}) the high diffusion barrier[83] could prevent these ions to enter the interlayer of the clay matrix and hence do not compete with $HgCl_4^{2-}$ for the effective adsorption sites. At higher concentration (300 mg L^{-1}), the relaxation in this diffusion barrier leads to the competing ability of ions such as zinc, cobalt, cadmium, nickel, copper, and lead by forming their respective chlorocomplexes[39,74] thereby causing a decrease in the percentage adsorption of mercury. At the 300 mg L^{-1} level, ions such as bromide and iodide interfere by decreasing the adsorption of mercury. These ions compete with chloride for the effective adsorption sites in the clay matrix as well as the protonated amine, as their respective tetrabromo/iodomercurate(II) complexes. In acidic medium, it is also probable that bromide and iodide would be preferably oxidized which may further decrease the percentage adsorption of mercury. Similarly, anions such as sulfate and phosphate could also interfere by competing with chloride for the ion-pair formation with the protonated amine.

3.13. Application to Study the Removal of Mercury from a Coal Fly Ash Sample. Fly ash is an important source of mercury pollution generated in thermal power plants and comprises of fine particles that rise with the flue gases.[4] In addition to mercury, some of the major metallic constituents present in fly ash include aluminum, iron, manganese, chromium, arsenic, and lead.[84] The fly ash sample was collected from a thermal power plant. Five g of the sample was taken and pretreated using the $HF-HNO_3-H_2SO_4$ mixture,[84] the resulting mixture was filtered and made up to a known volume. Hg(II) was adsorbed on the column as tetrachloromercurate(II) anion with the organophilic clay adsorbent material. The adsorption of mercury was quantitative, and this was ascertained from the analysis of mercury in the aqueous phase using cold vapor atomic absorption technique. The amine modified clay adsorbent was effective in the removal of mercury from the fly ash sample, and, furthermore, the adsorbed mercury could also be desorbed quantitatively using thiourea. The concentration of mercury in the fly ash sample was found to be 0.23 ± 0.02 $\mu g\ g^{-1}$ obtained as the average of three replicate determinations.

3.14. Comparison with other Solid Phase Adsorbents. The efficacy of trioctylamine modified clay adsorbent was compared with regard to its adsorption capacity with some of the other solid phase adsorbent materials. The comparison given in Table 4 illustrates the fact that the trioctylamine modified clay adsorbent is very effective in the adsorption of mercury as its tetrachloromercurate(II) anion.

Table 4. Comparison of Adsorption Capacity with other Adsorbents

Sl. no.	adsorbent material	adsorption capacity (mg g^{-1})	reference
1	2-mercaptobenzothiazole treated natural clay	2.71	85
2	2-mercaptobenzimidazole- natural clay	102.49	86
3	4-aminoantipyrine immobilized bentonite	52.9	87
4	trioctylamine modified sodium montmorillonite	140.84	present work

4. CONCLUSIONS

In conclusion, this work has established the effectiveness of interaction between tetrachloromercurate (II) anion and trioctylamine in acidic medium. The sorption kinetics favors the pseudo second order kinetic model and a maximium adsorption

dx.doi.org/10.1021/ie3008693 | Ind. Eng. Chem. Res. 2012, 51, 11312−11327

capacity of 140.84 mg g^{-1} in concurrence with the Langmuir isotherm. The adsorption process is consistent with the mechanism involving the electrostatic interaction between the tetrachloromercurate(II) anion and the protonated amine in the clay. The thermodynamically favorable adsorption process is driven by negative enthalpy and entropy changes, respectively. The adsorbent material could be effectively regenerated using thiourea, and the method could be scaled to a sample volume of 800 mL. As low as 10 ppb of mercury could be effectively adsorbed in the column. Finally, the method has proved to be successful in the adsorption of mercury from coal fly ash, which is a vital source of mercury pollution.

AUTHOR INFORMATION

Corresponding Author

*Phone: +91 40 66303503. Fax: +91 40 66303998. E-mail: nrajesh05@gmail.com.

Notes

The authors declare no competing financial interest.

ACKNOWLEDGMENTS

The Department of Science and Technology (DST), New Delhi, India funded this work (Project No: SR/S1/IC- 42/2007). We are grateful to Central Electrochemical Research Institute (CECRI) Karaikudi, India, and Indian Institute of Technology Madras (Chennai), India for their valuable assistance in the adsorbent characterization.

REFERENCES

(1) Camel, V. Solid phase extraction of trace elements. *Spectrochim. Acta, Part B* **2003**, *58*, 1177−1233.

(2) Bhattacharyya, K. G.; Gupta, S. S. Adsorption of chromium(VI) from water by clays. *Ind. Eng. Chem. Res.* **2006**, *45*, 7232−7240.

(3) Chumchal, M. M.; Rainwater, T. R.; Osborn, S. C.; Roberts, A. P.; Abel, M. T; Cobb, G. P.; Smith, P. N; Bailey, F. C. Mercury speciation and biomagnification in the food web of caddo lake, Texas and Louisiana, USA, a subtropical fresh water ecosystem. *Environ. Toxicol. Chem.* **2011**, *30*, 1153−1162.

(4) Liu, Y.; Kelly, D. J.; Yang, H.; Lin, C. C. H.; Kuznicki, S. M.; Xu, Z. Novel regenerable sorbent for mercury capture from flue gases of coal-fired power plant. *Environ. Sci. Technol.* **2008**, *42*, 6205−6210.

(5) Vieira, R. S.; Beppu, M. M. Dynamic and static adsorption and desorption of Hg(II) ions on chitosan membranes and spheres. *Water Res.* **2006**, *40*, 1726−1734.

(6) Trager, R. US crackdown on mercury. *Chem. World* Feb **2012**, *9*, p 8.

(7) De Mendonça Fabrega, F.; Mansur, M. B. Liquid−liquid extraction of mercury(II) from hydrochloric acid solutions by Aliquat 336. *Hydrometallurgy* **2007**, *87*, 83−90.

(8) Mahmoud, M. E. Selective solid phase extraction of mercury(II) by silica gel-immobilized-dithiocarbamate derivatives. *Anal. Chim. Acta* **1999**, *398*, 297−304.

(9) Rajesh, N.; Gurulakshmanan., G. Solid phase extraction and spectrophotometric determination of mercury by adsorption of its diphenylthiocarbazone complex on an alumina column. *Spectrochim. Acta , Part A* **2008**, *69*, 391−395.

(10) Xiong, C.; Yao, C. Synthesis characterization and application of triethylenetetramine modified polystyrene resin in removal of mercury, cadmium and lead from aqueous solutions. *Chem. Eng. J.* **2009**, *155*, 844−850.

(11) Mercier, L.; Detellier, C. Preparation, characterization, and applications as heavy metals sorbents of covalently grafted thiol functionalities on the interlamellar surface of montmorillonite. *Environ. Sci. Technol.* **1995**, *29*, 1318−1323.

(12) Cestari, A. R.; Airoldi, C. Chemisorption on thiol-silicas: Divalent cations as a function of pH and primary amines on thiol-mercury adsorbed. *J. Colloid Interface Sci.* **1997**, *195*, 338−342.

(13) Das., S. K.; Das, A. R.; Guha., A. K. A study on the adsorption mechanism of mercury on *aspergillus versicolor* biomass. *Environ. Sci. Technol.* **2007**, *41*, 8281−8287.

(14) Wang, L.; Xing, R.; Liu, S.; Cai, S.; Yu., H.; Feng., J.; Li, R.; Li, P. Synthesis and evaluation of a thiourea-modified chitosan derivative applied for adsorption of Hg(II) from synthetic waste water. *Int. J. Biol. Macromol.* **2010**, *46*, 524−528.

(15) Mudasir; Raharjo, G.; Tahir, I.; Wahyuni, E. T. Immobilization of dithizone onto chitin isolated from prawn seawater shells (*P. merguensis*) and its preliminary study for the adsorption of Cd(II) ion. *J. Phys. Sci.* **2008**, *19*, 63−78.

(16) Kushwaha, S.; Sreedhar, B.; Padmaja, P. Sorption of phenyl mercury, methyl mercury, and inorganic mercury onto chitosan and barbital immobilized chitosan: Spectroscopic, potentiometric, kinetic, equilibrium, and selective desorption studies. *J. Chem. Eng. Data* **2010**, *55*, 4691−4698.

(17) Sun, C.; Ma, F.; Zhang, G.; Qu, R.; Zhang, Y. Removal of mercury ions from ethanol solution using silica gel functionalized with amino-terminated dendrimer-like polyamidoamine polymers: Kinetics and equilibrium studies. *J. Chem. Eng. Data* **2011**, *56*, 4407−4415.

(18) Ahmaruzzaman, M.; Gupta, V. K. Rice husk and its ash as low-cost adsorbents in water and wastewater treatment. *Ind. Eng. Chem. Res.* **2011**, *50*, 13589−13613.

(19) Zhang, Y.; Li, Q.; Sun, L.; Tang, R.; Zhai, J. High efficient removal of mercury from aqueous solution by polyaniline/humic acid nanocomposite. *J. Hazard. Mater.* **2010**, *175*, 404−409.

(20) Billinge, S. J. L.; Mckimmy, E. J.; Shatnawi, M.; Kim, H. J.; Petkov, V.; Wermeille, D.; Pinnavaia., T. J. Mercury binding sites in thiol-functionalized mesostructured silica. *J. Am. Chem. Soc.* **2005**, *127*, 8492−8498.

(21) Bootharaju, M. S.; Pradeep, T. Uptake of toxic metal ions from water by naked and monolayer protected silver nanoparticles: An X-ray photoelectron spectroscopic investigation. *J. Phys. Chem. C* **2010**, *114*, 8328−8336.

(22) Yin, M.; Li, Z.; Liu, Z.; Yang, X.; Ren, J. Magnetic self-assembled zeolite clusters for sensitive detection and rapid removal of mercury(II). *ACS Appl. Mater. Interfaces* **2012**, *4*, 431−437.

(23) Pancharoen, U.; Somboonpanya, S.; Chaturabul, S.; Lothongkum, A. W. Selective removal of mercury as $HgCl_4^{2-}$ from natural gas well produced water by TOA via HFSLM. *J. Alloys Compd.* **2010**, *489*, 72−79.

(24) Ojea-Jimenez, I.; Lopez, X.; Arbiol, J.; Puntes, V. Citrate-coated gold nanoparticles as smart scavengers for mercury(II) removal from polluted waters. *ACS Nano* **2012**, *6*, 2253−2260.

(25) Zeng, Q. H.; Yu, A. B.; Lu, G. Q. (Max).; Paul, D. R. Clay-based polymer nanocomposites: Research and commercial development. *J. Nanosci. Nanotechnol.* **2005**, *5*, 1574−1592.

(26) Kennedy oubagaranadin, J. U.; Murthy, Z. V. P. Adsorption of divalent lead on a montmorillonite- lllite type of clay. *Ind. Eng. Chem. Res.* **2009**, *48*, 10627−10636.

(27) Zeng, Q. H.; Wang, D. Z.; Yu, A. B.; Lu, G. Q. Synthesis of polymer−montmorillonite nanocomposites by *in situ* intercalative polymerization. *Nanotechnol.* **2002**, *13*, 549−553.

(28) Wilson, R.; Plivelic, T. S.; Ramya, P.; Ranganathaiah, C.; Kariduraganavar, M. Y.; Sivasankarapillai, A. K.; Thomas, S. Influence of clay content and amount of organic modifiers on morphology and pervaporation performance of EVA/clay nanocomposites. *Ind. Eng. Chem. Res.* **2011**, *50*, 3986−3993.

(29) Krishna, B. S.; Murthy, D. S. R.; Jai Prakash, B. S. Surfactant-modified clay as adsorbent for chromate. *Appl. Clay Sci.* **2001**, *20*, 65−71.

(30) Ahmad, M. B.; Hoidy, W. H.; Ibrahim, N. A. B.; Al-Mulla, E. A. J. Modification of montmorillonite by new surfactants. *J. Eng. Appl. Sci.* **2009**, *4*, 184−188.

(31) Dias Filho, N. L.; Do Carmo, D. R. Study of an organically modified clay: Selective adsorption of heavy metal ions and

voltammetric determination of mercury(II). *Talanta* **2006**, *68*, 919−927.
(32) Colilla, M.; Darder, M.; Aranda, P.; Ruiz-Hitzky, E. Amperometric sensors based on mercaptopyridine - montmorillonite intercalation compounds. *Chem. Mater.* **2005**, *17*, 708−715.
(33) Boufatit, M.; Ait-Amar, H. Removal of N, N dimethylaniline from a dilute aqueous solution by Na^+/ K^+ saturated montmorillonite. *Desalination* **2007**, *206*, 300−310.
(34) Mahadevaiah, N.; Venkataramani, B.; Jai Prakash., B. S. Interaction of chromate on surfactant modified montmorillonite: Breakthrough curve study in fixed bed columns. *Ind. Eng. Chem. Res.* **2008**, *47*, 1755−1759.
(35) Karunasagar, D.; Balarama Krishna, M. V.; Anjaneyulu, Y.; Arunachalam, J. Studies of mercury pollution in a lake due to a thermometer factory situated in a tourist resort: Kodaikkanal, India. *Environ. Pollut.* **2006**, *143*, 153−158.
(36) Abou-El-Sherbini, K. S.; Hassanien, M. M. Study of organically modified montmorillonite clay for the removal of copper(II). *J. Hazard. Mater.* **2010**, *184*, 654−661.
(37) Li, H.; Li, Z.; Liu, T.; Xiao, X.; Peng, Z.; Deng, L. A novel technology for biosorption and recovery hexavalent chromium in wastewater by bio-functional magnetic beads. *Bioresour. Technol.* **2008**, *99*, 6271−6279.
(38) Cook, D. The structure of aminopyrine salts. *Can. J. Chem.* **1965**, *43*, 3322−3329.
(39) Rajesh, N.; Krishna Kumar, A. S.; Kalidhasan, S.; Rajesh, V. Trialkylamine impregnated macroporous polymeric sorbent for the effective removal of chromium from industrial wastewater. *J. Chem. Eng. Data* **2011**, *56*, 2295−2304.
(40) Rajesh, N.; Hari, M. S. Spectrophotometric determination of inorganic mercury(II) after preconcentration of its diphenylthiocarbazone complex on a cellulose column. *Spectrochim. Acta, Part A* **2008**, *70*, 1104−1108.
(41) Guo, Y.; Yan, N.; Yang, S.; Liu, P.; Wang, J.; Qu, Z.; Jia, J. Conversion of elemental mercury with a novel membrane catalytic system at low temperature. *J. Hazard. Mater.* **2012**, *213-214*, 62−70.
(42) Khalil, H.; Mahajan, D.; Rafailovich, M. Polymer−montmorillonite clay nanocomposites. Part 1: Complexation of montmorillonite clay with a vinyl monomer. *Polym. Int.* **2005**, *54*, 423−427.
(43) Mishra, M.; Bora, J. J.; Goswamee, R. L. Improvement of the mechanical strength of alumina preforms by coating with montmorillonite/LDH gels. *Appl. Clay Sci.* **2011**, *53*, 8−14.
(44) Chang, P. H.; Li, Z.; Jiang, W. T.; Jean, J. S. Adsorption and intercalation of tetracycline by swelling clay minerals. *Appl. Clay Sci.* **2006**, *46*, 27−36.
(45) Brigatti, M. F.; Colonna, S.; Malferrari, D.; Medici, L.; Poppi, L. Mercury adsorption by montmorillonite and vermiculite: A combined XRD, TG-MS and EXAFS study. *Appl. Clay Sci.* **2005**, *28*, 1−8.
(46) Anirudhan, T. S.; Suchithra, P. S.; Divya, L. Adsorptive potential of 2-mercaptobenzimidazole-immobilized organophilic hydrotalcite for mercury(II) ions from aqueous phase and its kinetic and equilibrium profiles. *Water, Air, Soil Pollut.* **2009**, *196*, 127−139.
(47) De Canck, E.; Lapeire, L.; De Clercq, J.; Verpoort, F.; Van der Voort, P. New ultrastable mesoporous adsorbent for the removal of mercury ions. *Langmuir* **2010**, *26*, 10076−10083.
(48) Puanngam, M.; Unob, F. Preparation and use of chemically modified MCM-41 and silica gel as selective adsorbents for Hg(II) ions. *J. Hazard. Mater.* **2008**, *154*, 578−587.
(49) Behrens, S. H.; Grier, D. G. The charge of glass and silica surfaces. *J. Chem. Phys.* **2001**, *115*, 6716−6721.
(50) Gounder, R.; Iglesia, E. The roles of entropy and enthalpy in stabilizing ion-pairs at transition states in zeolite acid catalysis. *Acc. Chem. Res.* **2012**, *45*, 229−238.
(51) Yu, Y.; Addai-Mensah, J.; Losic, D. Functionalized diatom silica microparticles for removal of mercury ions. *Sci. Technol. Adv. Mater.* **2012**, *13*, 1−11.
(52) Boszke, L.; Glosinska, G.; Siepak, J. Some aspects of speciation of mercury in a water environment. *Pol. J. Environ. Stud.* **2002**, *11*, 285−298.
(53) Cichy, W.; Schlosser, S.; Szymanowski, J. Extraction and pertraction of phenol through bulk liquid membranes. *J. Chem. Technol. Biotechnol.* **2005**, *80*, 189−197.
(54) Cakara, D.; Kleimann, J.; Borkovec, M. Microscopic protonation equilibria of poly(amidoamine) dendrimers from macroscopic titrations. *Macromolecules* **2003**, *36*, 4201−4207.
(55) Malik, R.; Ramteke, D. S.; Wate, S. R. Physico chemical and surface characterization of the adsorbent prepared from groundnut shell by $ZnCl_2$ activation and its ability to adsorb colour. *Indian J. Chem. Technol.* **2006**, *13*, 319−328.
(56) Langmuir, I. The adsorption of gases on plane surface of glass, mica and platinum. *J. Am. Chem. Soc.* **1918**, *40*, 1361−1403.
(57) Hall, K. R.; Eagleton, L. C.; Acrivos, A.; Ver Meulen, T. Pore and solid diffusion kinetics in fixed- bed adsorption under constant pattern condition. *Ind. Eng. Chem. Fundam.* **1966**, *5*, 212−218.
(58) Freundlich, H. M. F. Over the adsorption in solution. *Z. Phys. Chem.* **1906**, *57*, 385−470.
(59) Srivastava, V.; Weng, C. H.; Singh, V. K.; Sharma, Y. C. Adsorption of nickel ions from aqueous solutions by nano alumina: Kinetic, mass transfer, and equilibrium studies. *J. Chem. Eng. Data* **2011**, *56*, 1414−1422.
(60) Redlich, O.; Peterson, D. L. A useful adsorption isotherm. *J. Phys. Chem.* **1959**, *63*, 1024−1026.
(61) Vasanth Kumar, K.; Porkodi, K.; Rocha, F. Comments on "Equilibrium and kinetic studies for the biosorption system of copper(II) ion from aqueous solution using Tectona grandis L. f. leaves powder". *J. Hazard. Mater.* **2007**, *146*, 428−429.
(62) Temkin, M. I. Adsorption equilibrium and the kinetics of processes on nonhomogeneous surfaces and in the interaction between adsorbed molecules. *Zh. Fiz. Chim.* **1941**, *15*, 296−332.
(63) Rengaraj, S.; Yeon, J. W.; Kim, Y.; Jung, Y.; Ha, Y. K.; Kim, W. H. Adsorption characteristics of Cu(II) onto ion exchange resins 252H and 1500H: Kinetics, isotherms and error analysis. *J. Hazard. Mater.* **2007**, *143*, 469−477.
(64) Elovich, S. Y.; Larinov, O. G. Theory of adsorption from solutions of nonelectrolytes on solid (I) equation adsorption from solutions and the analysis of its simplest form, (II) verification of the equation of adsorption isotherm from solutions. *Izv. Akad. Nauk. SSSR, Otd. Khim. Nauk* **1962**, *2*, 209−216.
(65) Ncibi, M. C. Applicability of some statistical tools to predict optimum adsorption isotherm after linear and non-linear regression analysis. *J. Hazard. Mater.* **2008**, *153*, 207−212.
(66) Mohan, D.; Sharma, R.; Singh, V. K.; Steele, P.; Pittman, C. U., Jr. Fluoride removal from water using bio-char, a green waste, low cost adsorbent: Equilibrium uptake and sorption dynamics modelling. *Ind. Eng. Chem. Res.* **2012**, *51*, 905−914.
(67) Giles, C. H.; Mckay, R. B. Adsorption of cationic basic dyes by fixed yeast cells. *J. Bacteriol.* **1965**, *89*, 390−397.
(68) Ho, Y. S. Review of second-order models for adsorption systems. *J. Hazard. Mater.* **2006**, *B136*, 681−689.
(69) Lagergren, S. Zur theorie der sogennanten adsorption geloster stoffe. *K. Sven. Vetenskapsakad. Handl.* **1898**, *24*, 1−39.
(70) Boparai, H. K.; Joseph, M.; O'Carroll, D. M. Kinetics and thermodynamics of cadmium ion removal by adsorption onto nanozerovalent iron particles. *J. Hazard. Mater.* **2011**, *186*, 458−465.
(71) Weber, W. J.; Morris, J. C. Kinetics of adsorption on carbon from solution. *J. Sanit. Eng. Div., Am. Soc. Civ. Eng.* **1963**, *89*, 31−60.
(72) Sengil, I. A.; Ozacar, M.; Turkmenler, H. Kinetic and isotherm studies of Cu(II) biosorption onto valonia tannin resin. *J. Hazard. Mater.* **2009**, *162*, 1046−1052.
(73) Swain, S. K.; Mishra, S.; Sharma, P.; Patnaik, T.; Singh, V. K.; Jha, U.; Patel, R. K.; Dey, R. K. Development of a new inorganic−organic hybrid ion-exchanger of zirconium(IV)−propanolamine for efficient removal of fluoride from drinking water. *Ind. Eng. Chem. Res.* **2010**, *49*, 9846−9856.
(74) Santhana Krishna Kumar, A.; Kalidhasan, S.; Rajesh, V.; Rajesh, N. Application of cellulose-clay composite biosorbent toward the effective adsorption and removal of chromium from industrial wastewater. *Ind. Eng. Chem. Res.* **2012**, *51*, 58−69.

(75) Zhang, Y.; Cremer, P. S. Interactions between macromolecules and ions: The Hofmeister series. *Curr. Opin. Chem. Biol.* **2006**, *10*, 658−663.
(76) Zhao, H. Are ionic liquids kosmotropic or chaotropic? An evaluation of available thermodynamic parameters for quantifying the ion kosmotropicity of ionic liquids. *J. Chem. Technol. Biotechnol.* **2006**, *81*, 877−891.
(77) Onyango, M. S.; Leswifi, T. Y.; Ochieng, A.; Kuchar, D.; Otieno, F. O.; Matsuda, H. Breakthrough analysis for water defluoridation using surface-tailored zeolite in a fixed bed column. *Ind. Eng. Chem. Res.* **2009**, *48*, 931−937.
(78) Arencibia, A.; Aguado, J.; Arsuaga, J. M. Regeneration of thiol-functionalized mesostructured silica adsorbents of mercury. *Appl. Surf. Sci.* **2010**, *256*, 5453−5457.
(79) Atkins, P.; Paula, J. D. *Elements of Physical Chemistry*; Oxford University Press: New York, 2005.
(80) Shade, C. W. Automated simultaneous analysis of monomethyl and mercuric Hg in biotic samples by Hg-thiourea complex liquid chromatography following acidic thiourea leaching. *Environ. Sci. Technol.* **2008**, *42*, 6604−6610.
(81) Cardiano, P.; Falcone, G.; Foti, C.; Sammartano, S. Sequestration of Hg^{2+} by some biologically important thiols. *J. Chem. Eng. Data* **2011**, *56*, 4741−4750.
(82) Zhang, L.; Goh, S.; Hu, X.; Crawford, R.; Yu, A. Removal of aqueous toxic Hg(II) by functionalized mesoporous silica materials. *J. Chem. Technol. Biotechnol.* **2012**, DOI: 10.1002/jctb.3771.
(83) Bibby, A.; Mercier, L. Mercury(II) ion adsorption behavior in thiol-functionalized mesoporous silica microspheres. *Chem. Mater.* **2002**, *14*, 1591−1597.
(84) Sushil, S.; Batra, V. S. Analysis of fly ash heavy metal content and disposal in three thermal power plants in India. *Fuel* **2006**, *85*, 2676−2679.
(85) Dias Filho, N. L.; Polito, W. L.; Gushikem, Y. Sorption and preconcentration of some heavy metals by 2-mercaptobenzothiazole-clay. *Talanta* **1995**, *42*, 1031−1036.
(86) Manohar, D. M.; Anoop Krishnan, K.; Anirudhan, T. S. Removal of mercury(II) from aqueous solutions and chlor-alkali industry wastewater using 2- mercaptobenzimidazole-clay. *Water Res.* **2002**, *36*, 1609−1619.
(87) Wang, Q.; Chang, X.; Li, D.; Hu, Z.; Li, R.; He, Q. Adsorption of chromium(III), mercury(II) and lead(II) ions onto 4-amino-antipyrine immobilized bentonite. *J. Hazard. Mater.* **2011**, *186*, 1076−1081.